

# miR-7a alleviates the maintenance of neuropathic pain through regulation of neuronal excitability

Atsushi Sakai,<sup>1</sup> Fumihito Saitow,<sup>1</sup> Noriko Miyake,<sup>2</sup> Koichi Miyake,<sup>2</sup> Takashi Shimada<sup>2</sup> and Hidenori Suzuki<sup>1</sup>

1 Department of Pharmacology, Nippon Medical School, 1-1-5 Sendagi, Bunkyo-ku, Tokyo 113-8602, Japan

2 Department of Biochemistry and Molecular Biology, Nippon Medical School, 1-1-5 Sendagi, Bunkyo-ku, Tokyo 113-8602, Japan

Correspondence to: Hidenori Suzuki, MD, PhD,  
Department of Pharmacology,  
Nippon Medical School,  
1-1-5 Sendagi,  
Bunkyo-ku,  
Tokyo 113-8602,  
Japan  
E-mail: hsuzuki@nms.ac.jp

Neuronal damage in the somatosensory system causes intractable chronic neuropathic pain. Plastic changes in sensory neuron excitability are considered the cellular basis of persistent pain. Non-coding microRNAs modulate specific gene translation to impact on diverse cellular functions and their dysregulation causes various diseases. However, their significance in adult neuronal functions and disorders is still poorly understood. Here, we show that miR-7a is a key functional RNA sustaining the late phase of neuropathic pain through regulation of neuronal excitability in rats. In the late phase of neuropathic pain, microarray analysis identified miR-7a as the most robustly decreased microRNA in the injured dorsal root ganglion. Moreover, local induction of miR-7a, using an adeno-associated virus vector, in sensory neurons of injured dorsal root ganglion, suppressed established neuropathic pain. In contrast, miR-7a overexpression had no effect on acute physiological or inflammatory pain. Furthermore, miR-7a downregulation was sufficient to cause pain-related behaviours in intact rats. miR-7a targeted the  $\beta 2$  subunit of the voltage-gated sodium channel, and decreased miR-7a associated with neuropathic pain caused increased  $\beta 2$  subunit protein expression, independent of messenger RNA levels. Consistently, miR-7a overexpression in primary sensory neurons of injured dorsal root ganglion suppressed increased  $\beta 2$  subunit expression and normalized long-lasting hyperexcitability of nociceptive neurons. These findings demonstrate miR-7a downregulation is causally involved in maintenance of neuropathic pain through regulation of neuronal excitability, and miR-7a replenishment offers a novel therapeutic strategy specific for chronic neuropathic pain.

**Keywords:** hyperexcitability; microRNA; neuropathic pain; primary sensory neuron; voltage-gated sodium channel  $\beta 2$  subunit

**Abbreviations:** AAV = adeno-associated virus; DRG = dorsal root ganglion; EGFP = enhanced green fluorescent protein

## Introduction

Lesions or diseases of the somatosensory system cause severe chronic neuropathic pain as seen in cancers, herpes zoster, diabetes or traumatic nerve injury (O'Connor and Dworkin, 2009).

Plastic changes in peripheral and central neurons transmitting nociceptive information are considered the cellular basis for persistent pain, although the underlying molecular mechanisms for the initiation and maintenance phases of neuropathic pain are possibly distinct (Ji and Strichartz, 2004). Unfortunately, in marked contrast

to inflammatory pain, chronic neuropathic pain is poorly controlled by conventional analgesics, such as non-steroidal anti-inflammatory drugs and opioids (O'Connor and Dworkin, 2009). In developing novel analgesics effective for neuropathic pain, it is important to determine the disease stage- and pain type-specific molecular mechanisms. Dorsal root ganglion (DRG) neurons, primary sensory neurons that detect both innocuous and noxious stimuli and transmit signals to the spinal dorsal horn are an important analgesic target. In clinical practice, DRG neurons are the primary origin of neuropathic pain, and are involved in both initiation and maintenance of the pain state (Yoon *et al.*, 1996; Devor, 2006; Takahashi *et al.*, 2010).

MicroRNAs are genome-encoded non-coding RNAs, consisting of ~22 nucleotides in their mature form. microRNAs inhibit translation of specific genes in a sequence-dependent manner via recognition of the 3'-UTR sequence of target messenger RNAs (Bartel, 2009). Therefore, microRNAs have a significant impact on diverse cellular functions and are involved in a number of diseases, including cancer (Sayed and Abdellatif, 2011). In addition, extensive species conservation of microRNAs and their target sequences, suggests they are functionally important (Friedman *et al.*, 2009). However, their physiological and/or pathological roles in the nervous system remain poorly elucidated (McNeill and Van Vactor, 2012).

Recently, microRNAs expressed in the DRG were implicated as potential pain modulators (Niederberger *et al.*, 2011). In trigeminal ganglion neurons, microRNA expressions are differentially modulated following inflammatory muscle pain (Bai *et al.*, 2007). Deletion of *dicer*, the enzyme that produces mature microRNAs through cleavage of pre-microRNAs, attenuates inflammatory pain in nociceptive DRG neurons (Zhao *et al.*, 2010). Several groups have shown widespread microRNA expression changes induced in the DRG at various time points after peripheral nerve injury (Kusuda *et al.*, 2011; von Schack *et al.*, 2011; Zhang *et al.*, 2011; Zhou *et al.*, 2011). Furthermore, certain microRNAs are reportedly expressed in nociceptive DRG neurons and are predicted to modulate sodium channel expressions (Zhao *et al.*, 2010). Nevertheless, to date, the role of specific microRNAs in DRG neurons has not been investigated. Here, we identify miR-7a as an important microRNA for normal nociception. We also show that miR-7a dysfunction underlies maintenance of neuropathic pain through regulation of DRG neuronal excitability.

## Materials and methods

### Animal models

Male Sprague–Dawley rats (5 weeks) were used for all experiments. All experimental procedures were approved by our Institutional Committee on Laboratory Animals (Approval number, 23-107) and performed in accordance with the guidelines of the International Association for the Study of Pain (Zimmermann, 1983). Animals were singly housed and allowed food and water *ad libitum*. All surgeries were performed on rats under deep anaesthesia after intraperitoneal administration of sodium pentobarbital (50 mg/kg), except for intraplantar injections of complete Freund's adjuvant under isoflurane anaesthesia (1.5%). To create neuropathic pain models, lumbar fifth

(L5) spinal nerve ligation or chronic constriction injury of the sciatic nerve was performed (Bennett and Xie, 1988; Kim and Chung, 1992). For spinal nerve ligation, the left L5 spinal nerve was exposed and tightly ligated with 4-0 silk thread in two regions separated by ~1 mm. For chronic constriction injury, the left sciatic nerve was loosely ligated in four regions. For sham operations, the L5 spinal nerve was exposed but not ligated. For a model of inflammatory pain, rats were injected with complete Freund's adjuvant solution (100 µl; Sigma-Aldrich) into the left plantar skin of the hindpaw innervated by L5 DRG neurons as well as lumbar fourth (L4) and lumbar sixth DRG neurons, using a 1 ml syringe with a 26-gauge needle. The right side was left intact as a control.

### MicroRNA microarray

Total RNA was isolated using RNAiso Plus (Takara Bio). RNA quality was checked using the Agilent RNA 6000 Nano Kit and Agilent 2100 Bioanalyser (Agilent Technologies). Samples with a RNA integrity number ~9.0 were used for subsequent procedures. Total RNA (100 ng) was labelled with cyanine 3-cytidine bisphosphate using T4 RNA ligase (GE Healthcare) and miRNA Labelling Reagent and Hybridization Kit (Agilent Technologies). After purification, samples were hybridized to a rat microRNA microarray (Agilent Technologies) at 20 rpm, 55°C for 20 h. Fluorescent images of microarray slides were scanned using a DNA Microarray Scanner (Agilent Technologies). The fluorescent intensity of each spot was quantified using Feature Extraction software (Agilent Technologies) and signal intensities > 10, were considered positive expression. Data obtained were analysed using GeneSpring GX software (Agilent Technologies).

### Behavioural tests

The paw withdrawal response to mechanical stimuli was measured using a set of von Frey filaments (Muromachi Kikai). Each rat was placed on a metallic mesh floor covered with a plastic box, and a von Frey monofilament was applied from below the mesh floor to the plantar surface of the hind paw. The weakest force (g) inducing withdrawal of the stimulated paw, at least three times in five trials, was referred to as the paw withdrawal threshold. The Plantar Test (Ugo Basile) was used to examine thermal hyperalgesia. Each rat was placed on a glass plate with a radiant heat generator below. The average latency of paw withdrawal from the heat stimulus was measured twice, separated by a 5 min interval. Both tests were performed in a blind fashion.

### Reverse transcription-polymerase chain reaction

For quantitative analysis, all procedures were basically performed according to the manufacturers' protocols. Total RNA (10 ng) was reverse-transcribed using a mature miR-7a-specific stem-loop primer, included in the TaqMan<sup>®</sup> MicroRNA Assays (Life Technologies), using a TaqMan<sup>®</sup> MicroRNA Reverse Transcription Kit (Life Technologies). PCR mixtures were prepared using TaqMan<sup>®</sup> Universal PCR Master Mix, with premixed TaqMan<sup>®</sup> probe and a miR-7a-specific primer pair (included in TaqMan<sup>®</sup> MicroRNA Assays). For quantitative analysis of *Scn2b*, which encodes voltage-gated sodium channel β2 subunit, and *Gapdh* messenger RNA expression, total RNA (500 ng) was reverse-transcribed using iScript<sup>™</sup> select complementary DNA Synthesis Kit (Bio-Rad Laboratories) with a random primer. PCR amplification was performed with TaqMan<sup>®</sup> Gene Expression Master Mix and

premixed probe, and specific primer pairs for *Scn2b* or *Gapdh* (Life Technologies). The amplification efficiency per single PCR cycle was obtained by assaying serially-diluted samples (four points at 1:5 dilution), relative expression was calculated. For enhanced green fluorescent protein (EGFP) expression, PCR amplifications were performed at 94°C for 2 min, followed by 94°C for 30 s, 58°C (EGFP) or 50°C (*Actb*) for 30 s and 72°C for 90 s using appropriate forward and reverse primer pairs for EGFP (forward, 5'-ACACCCTGGTGAACCCGATCGAGCTGAAGG-3'; reverse, 5'-CCAGCAGGACCATGTGATCGCGCTTCTCGT-3') or *Actb* (forward, 5'-CCATGGATGACGATATCGCT-3'; reverse, 5'-ACGCACGATTCCCTCTCA-3'). Amplified PCR products were electrophoresed on 1.5% (w/v) agarose gels and stained with ethidium bromide. Agarose gel images were captured using a BioDoc-It® System UV Transilluminator (BM Equipment).

## In situ hybridization

Rats were deeply anaesthetized with intraperitoneal pentobarbital and perfused transcardially with PBS (pH 7.4) followed by fresh 4% paraformaldehyde in PBS. DRGs were removed and post-fixed in paraformaldehyde overnight, and then cryoprotected in 20% sucrose in PBS overnight. Next, they were rapidly frozen in dry ice/acetone and sectioned (10 µm) using a cryostat (Leica). miR-7-specific and negative control locked nucleic acid-modified DNA probes, conjugated with digoxigenins at 3' and 5' terminals, were obtained from Exiqon. Tissue was pretreated with 1 µg/ml proteinase K (Merck) at 37°C for 5 min, acetylated in 0.25% acetic acid in 0.1 M triethanolamine, and then hybridized with probes (50 nM) in hybridization buffer [50% formamide, 10% dextran sulphate, 5 × SSC (saline–sodium citrate; pH 7.0), 1 × Denhardt's solution and 150 µg/ml yeast RNA] at 50°C overnight. Slides were rinsed with wash buffer [50% formamide, 5 × SSC (pH 7.0) and 1% SDS] at 50°C for 30 min, and subsequently washed three times with a second wash buffer (50% formamide and 2 × SSC, pH 7.0) at 50°C for 30 min each wash. Slides were then incubated with 0.5% blocking solution (Roche Diagnostics) at room temperature for 1 h, and then with a sheep anti-digoxigenin antibody conjugated to alkaline phosphatase (Roche Diagnostics) at 4°C overnight. Slides were stained with BM purple alkaline phosphatase substrate solution (Roche Diagnostics) containing 2 mM levamisole, at room temperature for 7 days. Negative control probes did not produce any signal in intact L5 DRGs (data not shown), confirming sequence-specific staining. For measuring cell sizes of DRG neurons, four DRG sections (minimum separation, 60 µm) obtained from individual rats were analysed using Scion Image Beta 4.03. Quantitative analysis was performed in a blind fashion.

## Plasmids

To express mature rno-miR-7a, sequence including rno-miR-7a sequence was amplified from the rat genome using forward (5'-CCATGGTGTTCCTCGTCACT-3') and reverse (5'-CTGCGTTTTCAGCACCATC-3') primers, with EcoRI restriction sites attached at 5' ends. For β2 subunit, coding sequence was amplified using forward (5'-ATGCACAGGGATGCTGGCT-3') and reverse (5'-TTACTTGGCGCCATCTTCCG-3') primers, from complementary DNA reverse-transcribed from rat DRG-derived total RNA using oligo (dT) primers (Life Technologies) and SuperScript® II reverse transcriptase (Life Technologies). Sequences were subcloned into the EcoRI site of pCDH-CMV-MCS-EF1-copGFP (pCDH; System Biosciences), which expresses the transgene and copGFP under the control of the CMV and EF1 promoters, respectively (pCDH-miR-7a). Plasmid vectors (pmiRZip), expressing miRZip antisense sequence that specifically

targets miR-7 (pmiRZip-anti-miR-7), and control miRZip (pmiRZipC), through the H1 promoter were obtained (System Biosciences). Adeno-associated virus (AAV) plasmids expressing miR-7a (pAAV-miR-7a) were constructed by replacing the EcoRI–EcoRI fragment (containing human α-galactosidase A complementary DNA) of the AAV plasmid pCAaGBE (Takahashi *et al.*, 2002), with the EcoRI PCR amplified rno-miR-7a sequence. The plasmid, pCAaGBE, contains the CAG promoter and EGFP gene driven by the B19 promoter. Another plasmid, pAAV-EGFP (Noro *et al.*, 2004), contains the EGFP gene driven by the CAG promoter, and was used as a control. To generate AAV plasmids expressing miRZip against miR-7 (pAAV-miRZip-anti-miR-7), or control miRZip (pAAV-miRZipC), BglII fragments of pmiRZip-anti-miR-7 or pmiRZipC were subcloned into the BglII site of pEGFP-N3 (Promega). Then, EcoRI fragments of pEGFP-N3-miRZip-anti-miR-7 or pEGFP-N3-miRZipC were subcloned into the EcoRI site of pCAaGBE.

The plasmid vector encoding firefly luciferase followed by *Scn2b* 3' UTR was constructed. The *Scn2b* 3' UTR sequence was amplified from rat DRG-derived complementary DNA. Forward (5'-CTTT CACGGTGCACAGAC-3') and reverse (5'-CCACCAAACAGGACGTAGA-3') primer pairs with SpeI restriction sites attached at 5' ends were used. The *Scn2b* 3'-UTR sequence was subcloned into the SpeI site (after the luciferase gene), of pMIR-REPORTER (pMIR-*Scn2b*-3'-UTR; Life Technologies). The miR-7a seed sequence within the *Scn2b* 3' UTR was mutated using QuikChange® II XL Site-Directed Mutagenesis Kit (Agilent Technologies) and the following primers: 5'-TGTGCCTCTTGCTGATGCAACCTTTATTGAAGCTTGCTG-3' and 5'-CAGCAAGCTTCAATAAAGGTTGACATCAGCAAGAGGCACA-3'.

## Adeno-associated virus vector production

Serotype 6 AAV vectors were produced using an adenovirus-free triple transfection method, as previously described (Kurai *et al.*, 2007). The AAV packaging (pRepCap 6as; kindly provided by Dr. DW Russell) (Rutledge *et al.*, 1998) and helper (pHelper; Agilent Technologies) plasmids were co-transfected into HEK293 cells at a ratio of 1:1:1 using calcium phosphate precipitation. Six hours after transfection, the medium was replaced by fresh culture medium and cells were incubated for 3 days at 37°C under 5% CO<sub>2</sub>. Cells were suspended in PBS and freeze–thawed three times. Cell debris was pelleted at 6000 rpm for 30 min at 4°C, and AAV vectors were purified by ammonium sulphate precipitation and iodixanol continuous gradient centrifugation. Titres of each AAV vector were determined by quantitative PCR. For use, each AAV vector was diluted with PBS to ~1 × 10<sup>14</sup> vector genomes (vg)/ml. AAV vectors (5 µl) were slowly injected into L5 DRG using a microsyringe with a 27-gauge needle after behavioural tests.

## Immunofluorescence

L5 DRG sections were pre-incubated in PBS containing 5% normal donkey serum and 0.2% Triton™ X-100 for 30 min, and then incubated with a rabbit anti-GFP antibody (1:1000; Life Technologies) at 4°C overnight. Sections were washed in PBS and then incubated with a secondary antibody labelled with Alexa Fluor® 488 (Life Technologies) at room temperature for 1 h. Images were captured using a high-resolution digital camera equipped with a computer (Olympus).

## Luciferase assay

Activities of firefly and *Renilla* luciferases were measured using the Dual-Glo<sup>®</sup> Luciferase Assay System (Promega). Briefly, 293T cells were seeded onto a 96-well plate ( $2 \times 10^4$  cells per well). To assess anti-miR-7 efficiency, 293T cells were transfected with pmiRZip plasmid vectors, before transfection for luciferase assays. The next day, cells were co-transfected with pMIR-*Scn2b*-3'-UTR (16 ng), pGL4.74[hRLuc/TK] (100 ng; Promega) and pCDH-miR-7a (100 ng) using Lipofectamine<sup>®</sup> 2000 (Life Technologies). Two days after transfection, Dual-Glo<sup>®</sup> luciferase reagent was added to each well and firefly luminescence was measured using Wallac 1420 ARVO<sub>MX</sub> (PerkinElmer). Dual-Glo<sup>®</sup> Stop & Glo reagent was added to each well and *Renilla* luminescence was measured. Firefly luminescence was divided by *Renilla* luminescence, and then the luminescence of pMIR without *Scn2b* 3'-UTR for normalization.

## Immunoblotting

L4 and L5 DRGs, L5 dorsal root and L5 spinal nerve were obtained as described above. Tissues were sonicated in 10 mM Tris-HCl (pH 7.2) containing 250 mM sucrose, 10 mM HEPES, 10 mM EDTA and protease inhibitor cocktail (Roche Diagnostics). Homogenates were centrifuged at 12 000 rpm, 4°C for 20 min. Supernatants were electrophoresed on SDS-polyacrylamide gels (40 µg total protein per lane, except for 10 µg in β2 overexpression experiment) and electroblotted onto PVDF membranes (GE Healthcare). Membranes were incubated with anti-β2 subunit (1:500 or 1:1000; Millipore) or anti-GAPDH (1:1000; Cell Signaling Technology) antibody at 4°C overnight and then detected using horseradish peroxidase-conjugated secondary antibody (1:2000; Cell Signaling Technology) and chemiluminescence (ECL Western Blotting Detection Reagents or ECL Plus Western Blotting Detection Reagents; GE Healthcare). GAPDH was used as a loading standard. Optical densities of bands were quantified using Scion Image Beta 4.03.

## Electrophysiology

Compound action potentials were recorded from isolated dorsal roots using a suction electrode, as previously described (Stys *et al.*, 1991; Thakor *et al.*, 2009). A L5 DRG with dorsal root and spinal nerve attached, was removed and maintained in artificial CSF (138.6 mM NaCl, 3.35 mM KCl, 2.0 mM CaCl<sub>2</sub>, 1.3 mM MgCl<sub>2</sub>, 21.0 mM NaHCO<sub>3</sub>, 0.6 mM NaH<sub>2</sub>PO<sub>4</sub>, and 10.0 mM glucose) bubbled with 95% O<sub>2</sub>/5% CO<sub>2</sub> gas. After recovery from postoperative damage and attaining an equilibrium state (> 60 min), the L5 dorsal root was trimmed, transferred to a recording chamber and perfused continuously with oxygenated artificial CSF at a flow rate of 3.5 ml/min, at room temperature. Compound action potentials were amplified by MultiClamp 700B (Molecular Devices) in the AC mode. Stimulation was performed using bipolar tungsten electrodes at 0.05 Hz with durations of 0.12 ms and 0.5 ms, for A- and C-fibres, respectively. The stimulus pulse was delivered by an isolator (AMPI). Stimulation strength was increased stepwise at intervals of 20 s. Compound action potential amplitudes were measured peak-to-peak. Conduction velocity was calculated by dividing the latency to reach peak amplitude by the distance between stimulating and recording electrodes.

## Statistical analysis

Values are expressed as mean ± SEM. SPSS software (IBM) was used for statistical analyses. Normality of data was assessed by the

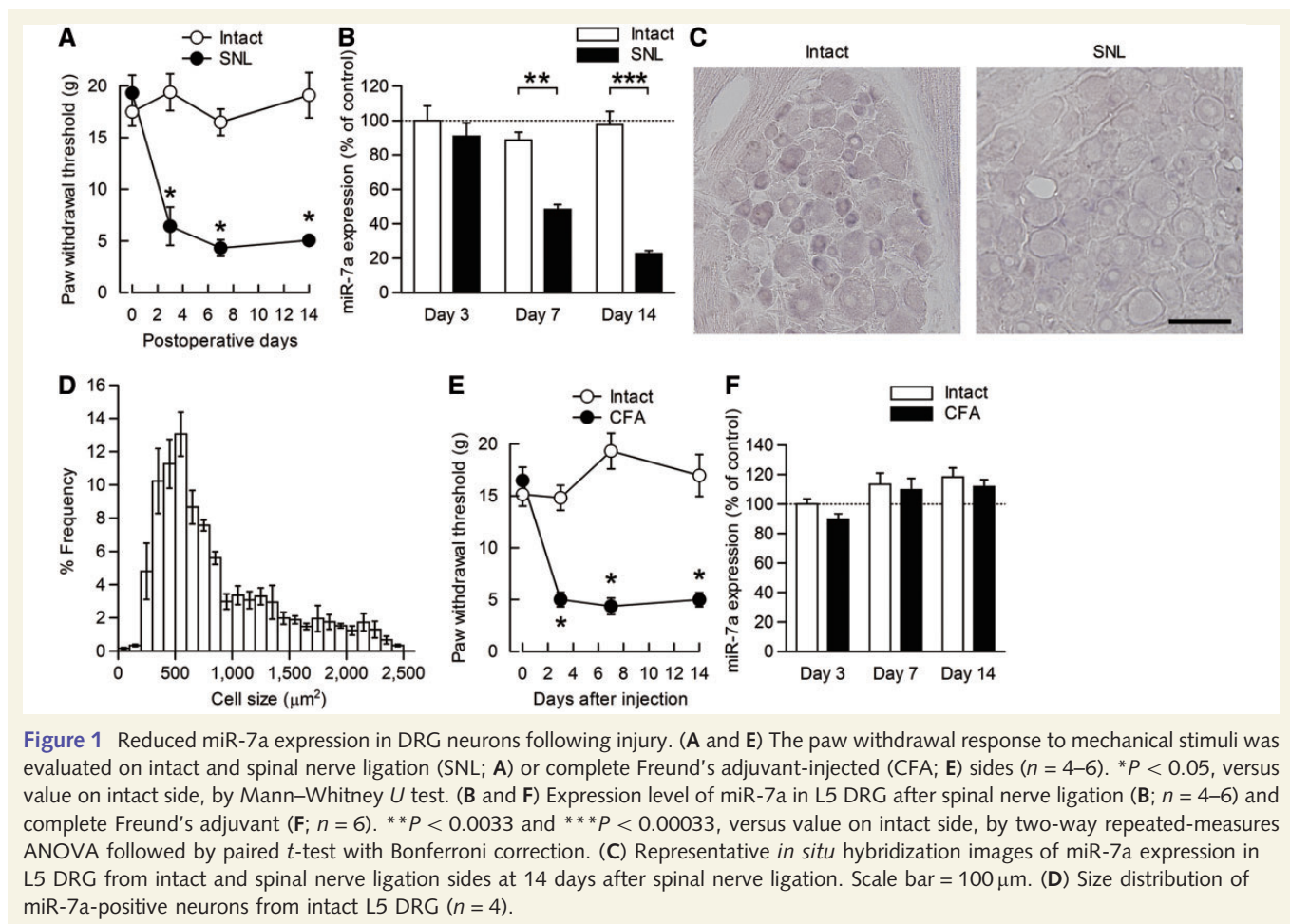
Shapiro-Wilk test. The paired *t*-test was used for normally distributed datasets, and the Mann-Whitney *U* test if normality was rejected. Equality of variance was assessed by Levene's test. Welch's or unpaired *t*-test was used, depending if the homogeneity of variance was rejected or not rejected, respectively. Differences between groups were assessed using two-way repeated-measures ANOVA. Expression changes with time were analysed with two-way repeated-measures ANOVAs followed by *post hoc* Bonferroni tests. All tests were two-tailed and values of  $P < 0.05$  were considered statistically significant.

## Results

### miR-7a is downregulated in neurons of injured dorsal root ganglion in the late phase of neuropathic pain

To identify microRNAs responsible for maintenance of neuropathic pain, we performed a microRNA microarray analysis using DRGs isolated from rats subjected to selective L5 spinal nerve ligation, a well-characterized neuropathic pain model (Kim and Chung, 1992). At 14 days after spinal nerve ligation when neuropathic pain was already established (Fig. 1A), a broad range of microRNA expressions were changed in the injured L5 DRG, compared to sham operation (Supplementary Fig. 1A and Supplementary Table 1). In marked contrast, no microRNAs exhibited significant expression changes in the neighbouring uninjured L4 DRG (Supplementary Fig. 1B and Supplementary Table 2), although both injured and neighbouring uninjured DRGs are implicated in neuropathic pain (Yoon *et al.*, 1996; Obata *et al.*, 2003; Fukuoka *et al.*, 2012). Among the microRNAs showing significant expression changes (Supplementary Table 1), miR-7a was most robustly reduced, therefore we chose to analyse miR-7a expression and function.

Although neuropathic pain developed almost immediately following spinal nerve ligation (Fig. 1A), the molecular mechanisms between early development and late maintenance of neuropathic pain differ considerably (Ji and Strichartz, 2004). Time course analysis using quantitative reverse transcription-PCR showed that 3 days after spinal nerve ligation, in the early phase of neuropathic pain, miR-7a expression was not altered (Fig. 1B). However, by the late phase of neuropathic pain, miR-7a expression gradually declined [ $F(1,13) = 93.06$ ,  $P < 0.001$  by two-way repeated-measures ANOVA]. In contrast, miR-7a expression in uninjured L4 DRG and L5 dorsal spinal cord did not change (Supplementary Fig. 2). We also examined miR-7a expression in L5 DRG after chronic constriction injury, another neuropathic pain model. When neuropathic pain was established at Day 14, miR-7a expression was also decreased (Supplementary Fig. 3). Next, we determined the miR-7a expression profile in L5 DRG neurons, as both nociceptive and non-nociceptive DRG neurons contribute to neuropathic pain (Todd, 2010). *In situ* hybridization revealed miR-7a was strongly expressed in small neurons, comprising putative nociceptors with slow conduction velocity, whereas most medium nociceptive and large non-nociceptive neurons had lower amounts of miR-7a (Fig. 1C and D). In the injured L5 DRG, miR-7a expression



decreased, and it became difficult to distinguish miR-7a-positive and -negative neurons of any cell size at 14 days after spinal nerve ligation (Fig. 1C). We also examined miR-7a expression in inflammatory pain, another subchronic pain syndrome distinct from neuropathic pain but with partially shared molecular mechanisms (Ren and Dubner, 2010). Expression of miR-7a in L5 DRG was unaltered after induction of inflammatory pain by complete Freund's adjuvant injection (Fig. 1F), although the extent of allodynia was comparable to that in neuropathic pain (Fig. 1A and E).

## miR-7a overexpression alleviates the late phase of neuropathic pain

To assess the direct contribution of miR-7a to neuropathic pain, we induced miR-7a expression specifically in L5 DRG neurons using a recombinant serotype 6 AAV vector, with EGFP as an expression marker (miR-7a AAV vector). Following direct injection of control (Fig. 2A) or miR-7a (Supplementary Fig. 4A) AAV vector into intact L5 DRG, EGFP expression was observed after 7 days in injected L5 DRG neurons of all cell sizes, as described previously (Towne et al., 2009). In contrast, EGFP expression was hardly detected in uninjected ipsilateral L4 and contralateral L5 DRGs (Supplementary Fig. 4B and C). No EGFP expression was detected in L5 dorsal spinal cord (Supplementary Fig. 4E). Seven

days after AAV vector injection, miR-7a expression was markedly increased above basal levels (Fig. 2B), and remained increased even after 21 days (Fig. 2B) in rats with spinal nerve ligation. Normal nociceptive responses were unaffected by miR-7a induction itself at 7 days after AAV vector injection (Fig. 2C). Whereas miR-7a overexpression did not affect the early phase of neuropathic pain, it alleviated both mechanical allodynia and thermal hyperalgesia in the late phase (Fig. 2C), indicating a specific contribution of miR-7a to maintenance, but not initiation, of, neuropathic pain. Furthermore, miR-7a-induced analgesia was still effective even after neuropathic pain was fully established (Fig. 2D). In contrast, miR-7a did not reverse inflammatory pain (Fig. 2E), implying a role for miR-7a in neuropathic pain.

## Functional blockade of miR-7a causes allodynia and hyperalgesia in intact rats

To test causal involvement of miR-7a in neuropathic pain, we blocked miR-7a function using anti-miR-7 miRZip, which competitively binds to mature miR-7 and inhibits its function. We confirmed anti-miR-7 effectively blocks miR-7a function *in vitro* (Fig. 6B). Next, we transduced anti-miR-7 to L5 DRG neurons in intact rats. Seven days after anti-miR-7 AAV vector injection, rats developed both mechanical allodynia and thermal hyperalgesia (Fig. 3). Thus, these

results show miR-7a is essential for normal pain sensation and its downregulation is sufficient to cause pathological pain.

## miR-7a targets the $\beta 2$ subunit of the voltage-gated sodium channel

MicroRNAs inhibit specific gene translation by binding to the 3'-UTR sequences of target messenger RNAs (Bartel, 2009). To identify miR-7a target genes relevant to neuropathic pain maintenance, we searched for potential candidate genes using TargetScan (<http://www.targetscan.org>). Among the candidates identified, we focused on the  $\beta 2$  subunit of the voltage-gated sodium channel complex, because it is upregulated in DRG neurons after nerve injury (Pertin *et al.*, 2005), and mice with a  $\beta 2$  subunit-null mutation exhibit less severe neuropathic pain (Pertin *et al.*, 2005). Therefore, we determined if *Scn2b* is actually a direct miR-7a target using luciferase assays. The *Scn2b* 3' UTR sequence (including predicted miR-7a target sequence), was inserted downstream of the firefly luciferase gene in a plasmid vector. Activity of luciferase with the *Scn2b* 3' UTR was attenuated by miR-7a (Fig. 4A). To identify the miR-7a binding sequence within the 3' UTR, we mutated the predicted seed sequence (Fig. 4B), and found miR-7a no longer decreased luciferase activity (Fig. 4A). Thus, miR-7a directly targets the *Scn2b* 3' UTR in a

sequence-specific manner. Moreover, the miR-7a-binding site is well conserved among mammals (Fig. 4B), indicating *Scn2b* regulation by miR-7a is functionally important.

## $\beta 2$ subunit protein increases in neuropathic pain independent of messenger RNA levels

Our results suggest miR-7a regulates  $\beta 2$  subunit expression, therefore we determined if expression of  $\beta 2$  subunit protein is upregulated in the late phase of neuropathic pain. At 7 and 14 days after spinal nerve ligation,  $\beta 2$  subunit protein was significantly increased in injured L5 DRG [ $F(1,15) = 56.46$ ,  $P < 0.001$  by two-way repeated-measures ANOVA; Fig. 5A], and its central and peripheral axons, dorsal root [ $F(1,14) = 97.05$ ,  $P < 0.001$  by two-way repeated-measures ANOVA; Fig. 5B] and spinal nerve [ $F(1,11) = 110.83$ ,  $P < 0.001$  by two-way repeated-measures ANOVA; Fig. 5C], respectively. Increases in  $\beta 2$  subunit protein are inversely correlated with miR-7a downregulation (Fig. 1B), and appear to be due to post-transcriptional regulation, as *Scn2b* messenger RNA expression was decreased or unchanged by spinal nerve ligation [ $F(1,9) = 20.79$ ,  $P = 0.0014$  by two-way repeated-measures ANOVA; Fig. 5D]. On the other hand, *Scn2b*

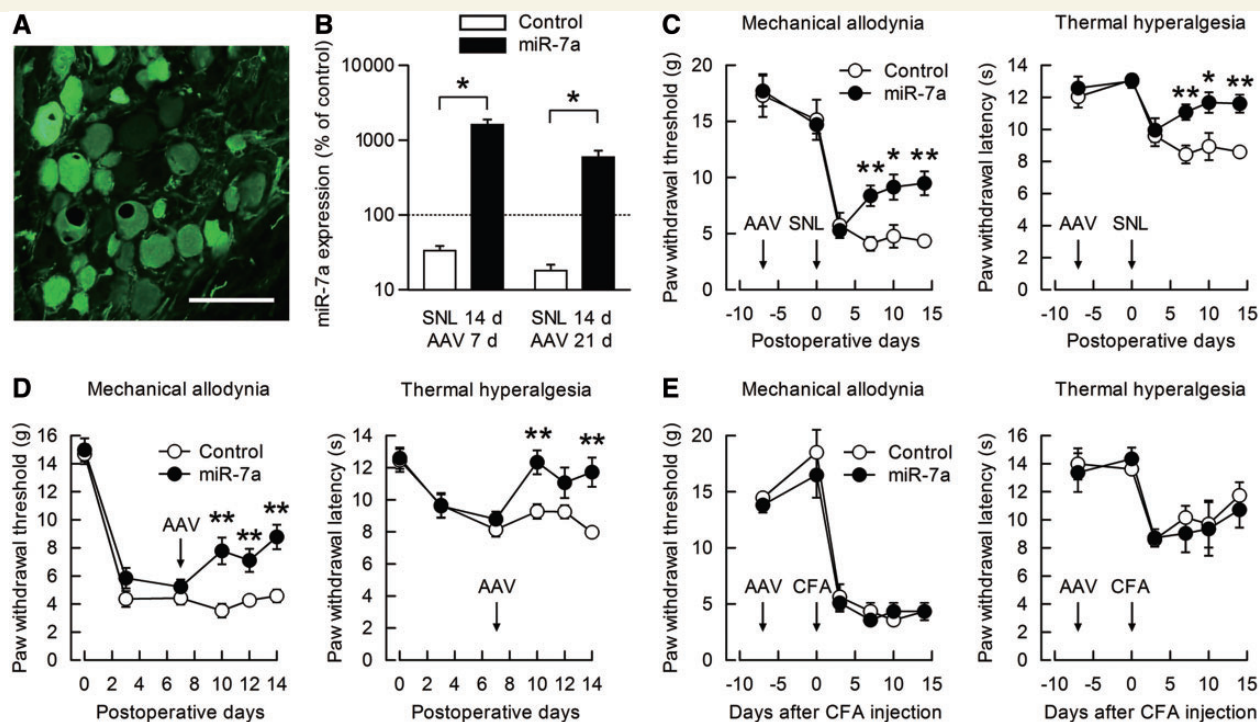


**Figure 2** miR-7a alleviates established neuropathic pain. (A) Representative image of EGFP immunofluorescence in an intact L5 DRG 7 days after injection of a control AAV vector. Scale bar = 100  $\mu$ m. (B) miR-7a expression levels in L5 DRG 14 days after spinal nerve ligation (SNL). Rats were injected with control or miR-7a AAV vector, 7 days after (AAV 7 d) or before (AAV 21 d) spinal nerve ligation ( $n = 3-4$ ). Values are expressed as percentages of values on the intact side. \* $P < 0.05$ , by Welch's  $t$ -test. (C-E) The paw withdrawal response to mechanical and thermal stimuli was evaluated on spinal nerve ligation (C and D;  $n = 6-10$ ) and complete Freund's adjuvant-injected (E;  $n = 3$ ) sides. Control or miR-7a AAV vector was injected 7 days before spinal nerve ligation (C) or complete Freund's adjuvant injection (E), or after spinal nerve ligation (D). \* $P < 0.05$  and \*\* $P < 0.01$ , versus value of control AAV injection, by Mann-Whitney  $U$  test for mechanical allodynia and unpaired  $t$ -test for thermal hyperalgesia.

messenger RNA and  $\beta 2$  subunit protein expression levels were unaltered in uninjured L4 DRG (Fig. 5E and Supplementary Fig. 5). Similarly,  $\beta 2$  subunit protein expression was not changed in inflammatory pain (Fig. 5F). Interestingly, 3 days after spinal nerve ligation, when miR-7a is not yet downregulated (Fig. 1B),  $\beta 2$  subunit protein was increased in L5 DRG and its axons (Fig. 5A–C), suggesting another regulatory mechanism operates in the early phase of neuropathic pain.

## The $\beta 2$ subunit is responsible for miR-7a-mediated analgesia of neuropathic pain

We further examined if miR-7a modulation affects  $\beta 2$  subunit protein expression. miR-7a overexpression suppressed  $\beta 2$  subunit

protein upregulation in injured L5 DRG (Fig. 6A). In addition, anti-miR-7, which blocked the miR-7a-induced decrease in activity of luciferase with the *Scn2b* 3' UTR (Fig. 6B), increased  $\beta 2$  subunit protein levels in L5 DRG of intact rats (Fig. 6C). This suggests the miR-7a and  $\beta 2$  subunit are co-expressed in the same DRG neurons, and miR-7a downregulation sufficiently causes upregulation of  $\beta 2$  subunit protein in the late phase of neuropathic pain. To further determine the role of the  $\beta 2$  subunit as an intermediate for miR-7a-induced analgesia, we induced  $\beta 2$  subunit expression simultaneously with miR-7a in L5 DRG of spinal nerve ligated rats. The  $\beta 2$  subunit-coding sequence without its original miR-7a target sequence was incorporated into an AAV vector to avoid miR-7a-mediated translational repression. In spinal nerve ligated rats injected with miR-7a and  $\beta 2$  subunit AAV vectors,  $\beta 2$  subunit protein expression remained upregulated (Fig. 6D). Moreover, in these rats, the neuropathic pain state was retained by  $\beta 2$  subunit expression despite co-injection with the miR-7a AAV vector (Fig. 6E). Thus, miR-7a downregulation causes neuropathic pain at least partly by regulating  $\beta 2$  subunit protein expression, although miR-7a also regulates expression of multiple other genes (Kefas *et al.*, 2008; Junn *et al.*, 2009; Fang *et al.*, 2012).

## miR-7a suppresses hyperexcitability of dorsal root ganglion neurons after nerve injury

Hyperexcitability of DRG neurons in response to neuronal damage contributes to both development and maintenance of neuropathic pain (Chung and Chung, 2002; Devor, 2006; Gold and Gebhart, 2010). In addition, the  $\beta 2$  subunit affects cell surface expression of voltage-gated sodium channels thereby increasing neuronal excitability (Isom *et al.*, 1995; Lopez-Santiago *et al.*, 2006). Thus, we examined compound action potentials from L5 C- and A-fibres, in the axons of small and medium-to-large DRG neurons,

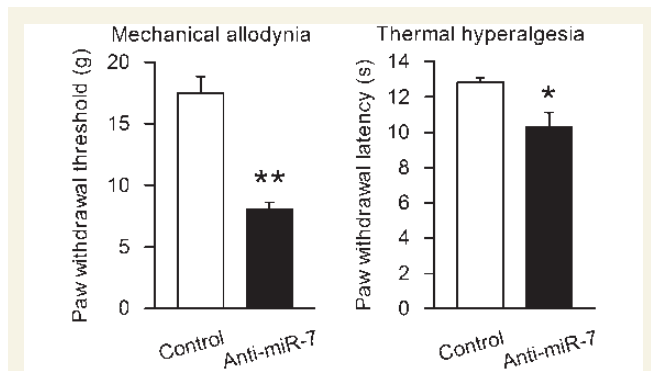


**Figure 3** Functional blockade of miR-7 in DRG neurons causes pain. The paw withdrawal response to mechanical and thermal stimuli was evaluated on AAV-injected sides ( $n = 5-6$ ). AAV vector encoding control or anti-miR-7 miRZip was injected into L5 DRG of intact rats 7 days before behavioural tests. \* $P < 0.05$  and \*\* $P < 0.01$ , versus value of control AAV injection, by Mann–Whitney  $U$  test for mechanical allodynia and unpaired  $t$ -test for thermal hyperalgesia.

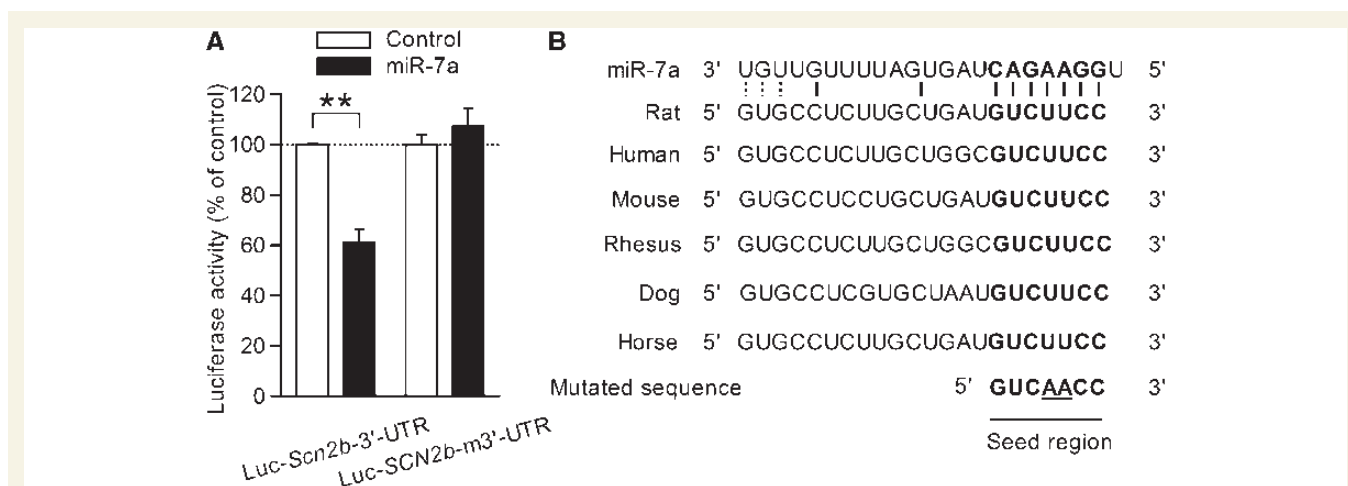


**Figure 4** miR-7a directly targets the *Scn2b* 3'-UTR. (A) Activity of luciferase with *Scn2b* 3' UTR or a mutated (m) 3' UTR in 293T cells co-transfected with control or miR-7a-expressing plasmid vector ( $n = 4$ ). \*\* $P < 0.01$ , by paired  $t$ -test. (B) Schematic representation of miR-7a sequence and its target sequence within the *Scn2b* 3' UTR. The target sequence is well conserved among mammals. The seed sequence is indicated by bold letters.

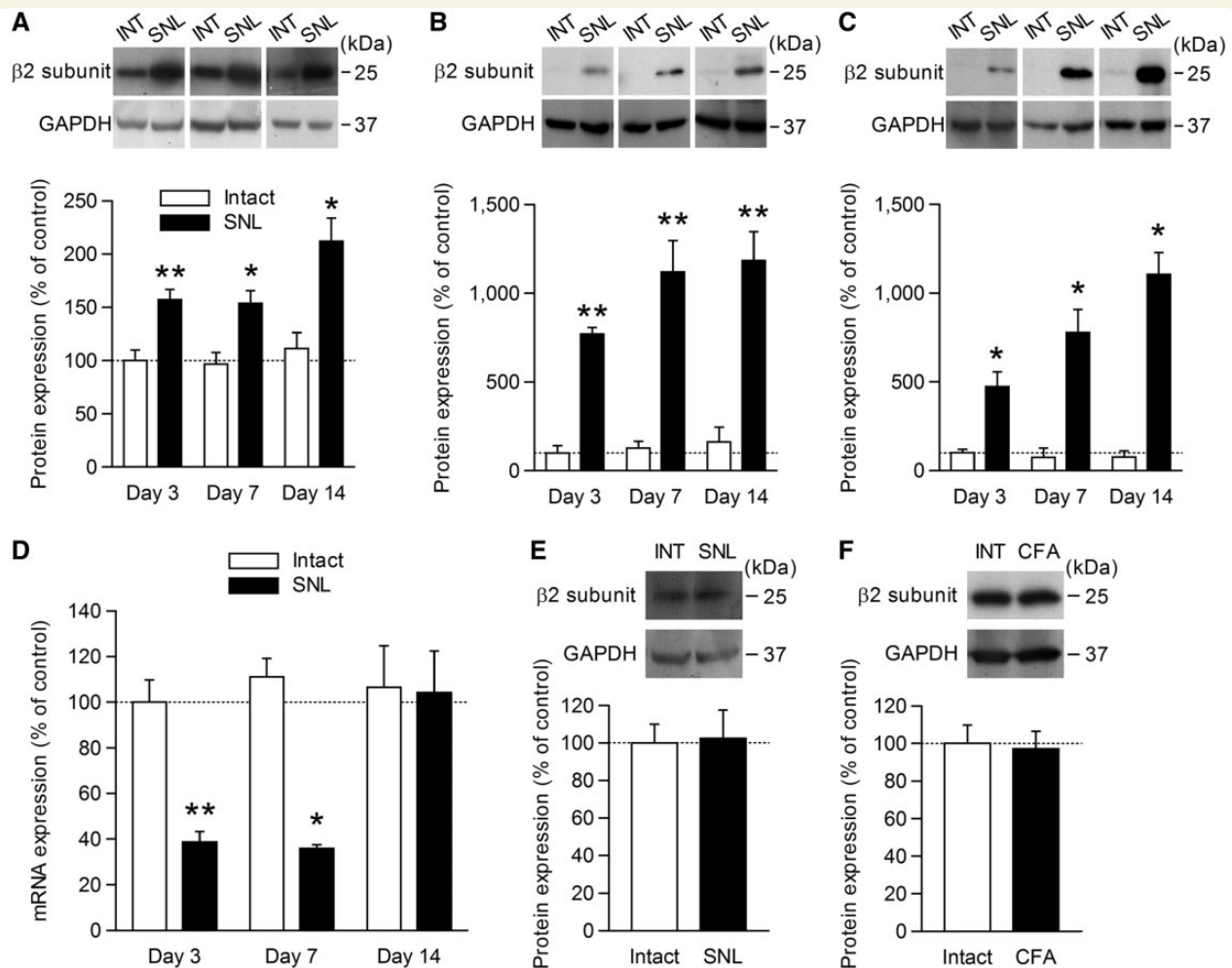


**Figure 5** β2 subunit protein is specifically upregulated in injured DRG independent of messenger RNA levels. (A–C) Expression level of β2 subunit protein in L5 DRG (A), dorsal root (B) and spinal nerve (C) from intact (INT) and spinal nerve ligation (SNL) sides after nerve injury ( $n = 4–7$ ). (D) Expression level of *Scn2b* messenger RNA in L5 DRG ( $n = 4$ ). (E) Expression level of β2 subunit protein in L4 DRG 14 days after spinal nerve ligation ( $n = 4$ ). (F) Expression level of β2 subunit protein in L5 DRG from intact and complete Freund's adjuvant-injected sides 14 days after complete Freund's adjuvant injection ( $n = 4$ ). GAPDH was used as a loading standard. Values are expressed as percentages of values on the intact side. \* $P < 0.0167$  and \*\* $P < 0.0033$ , by two-way repeated-measures ANOVA followed by paired  $t$ -test with Bonferroni correction.

respectively. The C- and A-fibre compound action potentials were distinguished by appropriate conduction velocities, which were unaffected by spinal nerve ligation (Supplementary Fig. 6). However, compound action potential amplitudes of C-, but not A-fibres, were increased at 14 days after spinal nerve ligation [ $F(1,14) = 19.07$ ,  $P < 0.001$  by two-way repeated-measures ANOVA; Fig. 7A–C], indicating increased excitability of small nociceptive DRG neurons. Decreased compound action potential amplitudes lead to analgesia in a variety of pain models, including neuropathic pain (Mert *et al.*, 2006; Gonçalves *et al.*, 2008; Guven *et al.*, 2011). Consistent with this, after spinal nerve ligation, miR-7a overexpression in L5 DRG neurons reduced increased C-fibre compound action potential amplitudes after spinal nerve ligation [ $F(1,11) = 5.59$ ,  $P = 0.038$  by two-way repeated-measures ANOVA; Fig. 7D and E]. A-fibre compound action potential amplitudes were also slightly, but not significantly, suppressed by

miR-7a (Fig. 7D and F). Thus, miR-7a suppressed increased excitability of nociceptive neurons in the injured DRG.

## Discussion

We have identified miR-7a as a key functional RNA for maintenance of neuropathic pain. miR-7a downregulation is causally involved in maintenance of neuropathic pain, and exogenous miR-7a specifically alleviated neuropathic pain. miR-7a targeted protein expression of the β2 subunit of voltage-gated sodium channel. Furthermore, miR-7a suppressed hyperexcitability of nociceptive DRG neurons, in association with decreased β2 subunit expression. Thus, microRNA-mediated translational regulation plays a significant role in the pathophysiology of chronic neuropathic pain, ranging from molecular and cellular changes in



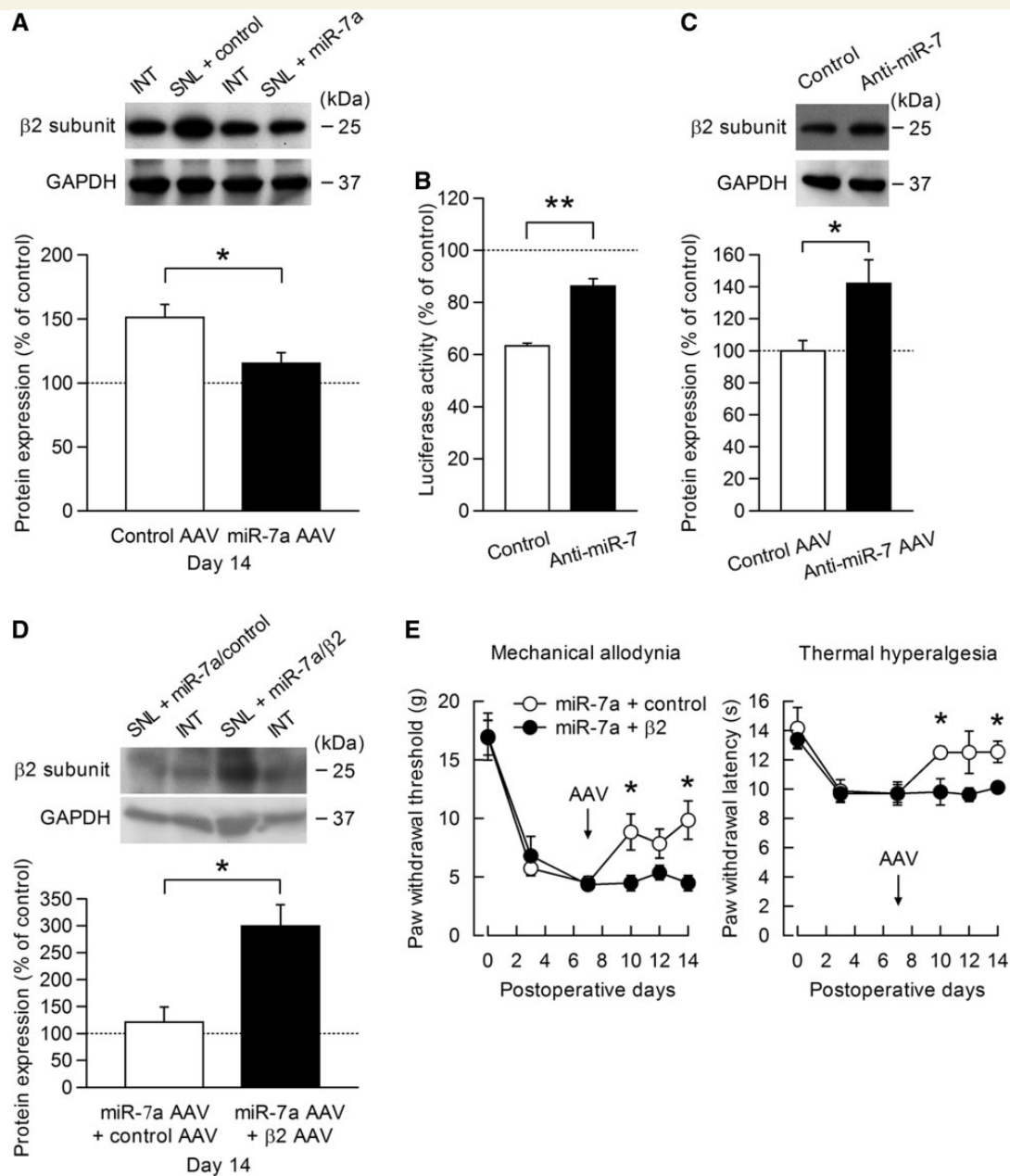


**Figure 6** The  $\beta 2$  subunit is responsible for miR-7a-induced analgesia. (A) Expression level of  $\beta 2$  subunit protein in L5 DRG from intact (INT) and spinal nerve ligation (SNL) sides 14 days after spinal nerve ligation. Control or miR-7a AAV vector was injected into L5 DRG 7 days after spinal nerve ligation ( $n = 5$ ). Values are expressed as percentages of values on the intact side. GAPDH was used as a loading standard. (B) Activity of luciferase with *Scn2b* 3' UTR, in 293T cells. In addition to the miR-7a-expressing plasmid vector, control or anti-miR-7 miRZip plasmid vector was transfected ( $n = 4$ ). (C) Expression level of  $\beta 2$  subunit protein in L5 DRG 7 days after injection of AAV vectors expressing control or anti-miR-7 miRZip ( $n = 5-6$ ). (D and E) The miR-7a AAV vector, in combination with AAV vector encoding either control or  $\beta 2$  subunit without original *Scn2b* 3'-UTR, was injected into L5 DRG 7 days after spinal nerve ligation. (D) Expression level of  $\beta 2$  subunit protein 14 days after spinal nerve ligation ( $n = 3$ ). Values are expressed as percentages of values on the intact side. (E) The paw withdrawal response to mechanical and thermal stimuli was evaluated on spinal nerve ligation sides ( $n = 5-6$ ). \* $P < 0.05$  and \*\* $P < 0.01$ , by Mann-Whitney  $U$  test for mechanical allodynia and unpaired  $t$ -test for  $\beta 2$  subunit expression, luciferase activity and thermal hyperalgesia.

neurons to behavioural output. Given that expression of many microRNAs are altered following nerve injury, widespread changes in gene expression at the translational step may contribute to functional alteration of primary sensory neurons in response to nerve injury.

In the present study, neuronal injury caused robust downregulation of miR-7a, which we have consequently shown to cause neuronal and behavioural disturbances. miR-7a is known to be an important regulator for determination of the dopaminergic phenotype during development (de Chevigny *et al.*, 2012), and is also

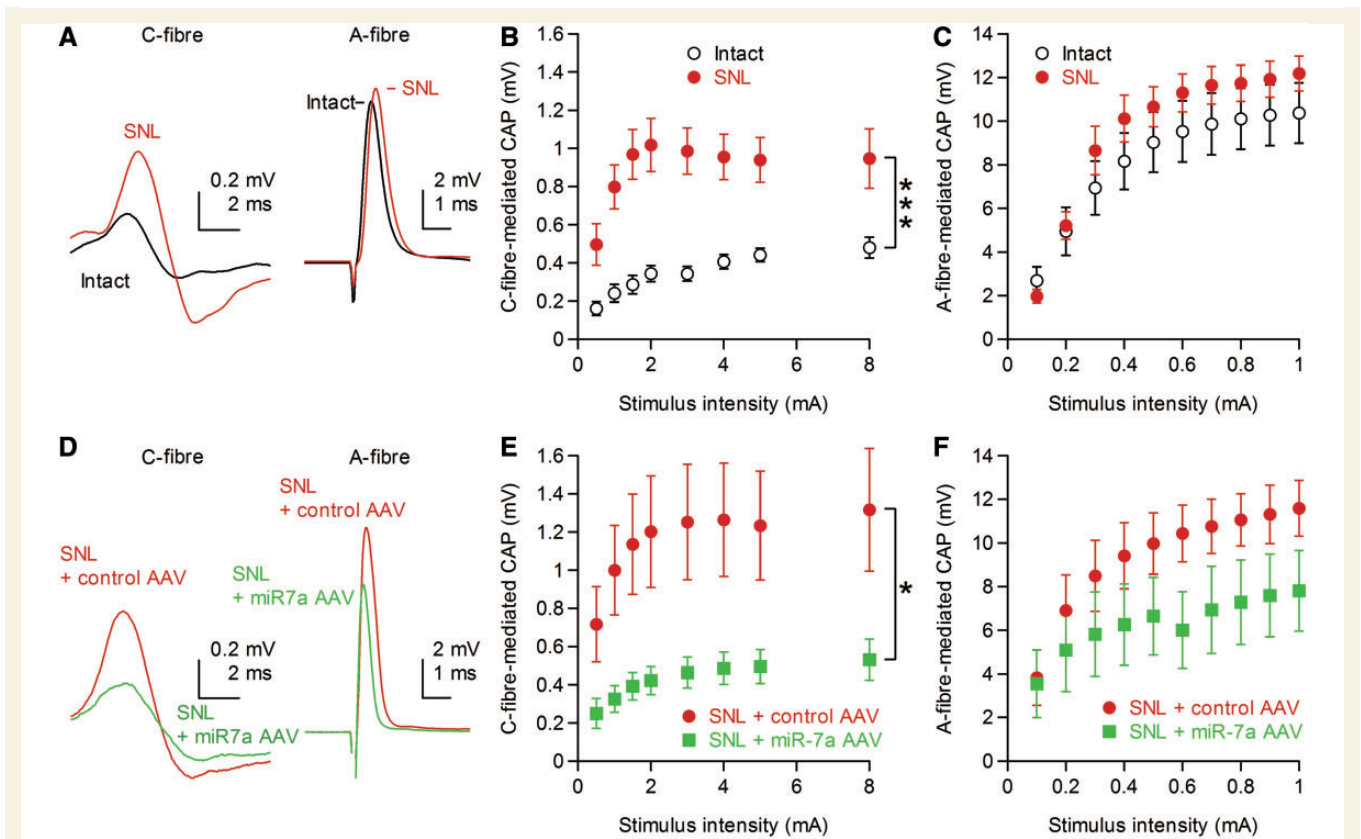


**Figure 7** miR-7a suppresses C-fibre hyperexcitability associated with nerve injury. (A and D) Superimposed images of representative compound action potential (CAP) traces from L5 dorsal roots on intact and spinal nerve ligation (SNL) sides (A), and from injured dorsal roots after control and miR-7a AAV vector injection (D), in response to maximum stimulus intensity. (B and C) Compound action potential amplitudes of C-fibres (B) and A-fibres (C) on intact and spinal nerve ligation sides 14 days after spinal nerve ligation ( $n = 8$ ). (E and F) Compound action potential amplitudes of C-fibres (E) and A-fibres (F) 14 days after spinal nerve ligation with control or miR-7a AAV vector injection at day 7 ( $n = 7$ ). \* $P < 0.05$  and \*\*\* $P < 0.001$ , by two-way repeated-measures ANOVA.

reported to decrease in a mouse model of Parkinson's disease (Junn *et al.*, 2009). In addition, pro-inflammatory interleukin-1 $\beta$ , which is involved in a variety of neurological disorders including Parkinson's disease, Alzheimer's disease, amyotrophic lateral sclerosis and multiple sclerosis (Ruggiero, 2012; Smith *et al.*, 2012), reportedly decreases miR-7 expression (Nguyen *et al.*, 2010). Thus, miR-7 downregulation may be commonly induced, and play a pivotal role in the pathophysiology of neurological diseases associated with degeneration and inflammation, as well as neuropathic pain.

miR-7a may be a preferable target for neuropathic pain treatment due to its selectivity in pain conditions. We found miR-7a specifically suppressed neuropathic pain, but not physiological and inflammatory pain. Although both inflammatory and neuropathic pain can take a chronic course, and partly share molecular mechanisms, they have distinct roles. Physiological and inflammatory pain is important as an alert system for organisms, to protect the body from potential damage and to prompt rest and healing. In contrast, chronic neuropathic pain is no longer beneficial, and thus fully pathological. Therefore, miR-7a is a preferable target for ensuring no effect on other pain conditions. In addition to its selective effect on neuropathic pain, miR-7a offers an advantage in alleviation of established chronic pain, consistent with progressive

decreases in miR-7a expression. In clinical settings, the ability to reverse established neuropathic pain may translate to increased clinical utility, as drug treatment is typically initiated after the onset of neuropathic pain.

*In situ* hybridization revealed widespread miR-7a expression in small DRG neurons, putative nociceptive neurons, as well as medium and large DRG neurons. Consistently, a study using mice with a small DRG neuron-specific dicer null mutation suggests miR-7a expression is present in small DRG neurons (Zhao *et al.*, 2010). Distribution of miR-7a expression appears to coincide with the  $\beta 2$  subunit, as  $\beta 2$  subunit protein is also increased in small to large DRG neurons after nerve injury (Pertin *et al.*, 2005). In addition, we found miR-7 functional blockade can increase  $\beta 2$  subunit protein expression. Overall, our results suggest that DRG neurons express both miR-7a and  $\beta 2$  subunit, and those that have reduced or lost miR-7a expression begin to increase  $\beta 2$  subunit protein expression in the same DRG neurons. Protein expression of the  $\beta 2$  subunit was upregulated, while *Scn2b* messenger RNA expression was downregulated or unchanged, consistent with the previous report by Pertin *et al.* (2005). Although the reason for decreased *Scn2b* messenger RNA at Days 3 and 7, yet unchanged at Day 14, after spinal nerve ligation, in our study is unknown,

discrepancies between the abundance of cognate protein and RNA molecules are frequently observed, including in the neuropathic pain state (Ji *et al.*, 2002; Pertin *et al.*, 2005). In the early phase of neuropathic pain, miR-7a expression was unchanged and miR-7a overexpression did not alleviate pain, suggesting involvement of other microRNAs and/or other mechanisms including upregulation of translational machinery and reduced degradation of  $\beta 2$  subunit protein. After nerve injury, protein synthesis can be modulated by ERK1/2 and p38 MAP kinase, which are activated in injured DRG neurons (Obata *et al.*, 2004). These MAP kinases increase eukaryotic translation initiation factor 4E (eIF4E) (Hou *et al.*, 2012), resulting in exaggerated cap-dependent translation (Santini *et al.*, 2013). In marked contrast to the early phase, our data clearly show that reduced function in miR-7a alone is sufficient to increase  $\beta 2$  subunit protein expression in the late phase of neuropathic pain. Therefore, miR-7a specifically plays an important role in protein expression modulation in the late phase of neuropathic pain.

Consistent with our finding showing the importance of the  $\beta 2$  subunit in pain modulation by miR-7a,  $\beta 2$  subunit-null mice show less severe neuropathic pain behaviours (Pertin *et al.*, 2005). However, miR-7a is reported to regulate expression of a variety of genes. For example, miR-7 protects cells against oxidative stress through downregulation of  $\alpha$ -synuclein (Junn *et al.*, 2009), and inhibits epidermal growth factor receptor and phosphoinositide 3-kinase/Akt signalling pathways (Kefas *et al.*, 2008; Fang *et al.*, 2012). Therefore, we cannot exclude the possibility that miR-7a target genes, other than the  $\beta 2$  subunit, are also involved in miR-7a-induced analgesia. Further insight into miR-7a function in neurons will improve our understanding of the pathophysiology of neuropathic pain.

Targeting the voltage-gated sodium channel is also a promising strategy to treat neuropathic pain, although current voltage-gated sodium channel blockers have significant adverse effects (Devor, 2006). Alternatively, gene therapy to suppress abnormal expression of a specific voltage-gated sodium channel,  $\text{Na}_v 1.3$ , ectopically expressed in DRG neurons after nerve injury, was recently reported to be effective, and avoided the side effects of voltage-gated sodium channel blockers (Samad *et al.*, 2013). Thus, miR-7a-induced normalization of neuronal excitation, rather than blockade with voltage-gated sodium channel blockers, also proves to be an effective route to treat established neuropathic pain with a peripheral origin. Excitability of small DRG neurons increases in response to nerve injury (Zhang *et al.*, 1997; Abdulla and Smith, 2001; Woolf and Ma, 2007; Thakor *et al.*, 2009), and increased excitability of injured DRG neurons contributes to both development and maintenance of neuropathic pain (Devor, 2006). In general, compound action potential amplitudes are increased with stronger stimulus intensities because of an increase in the number of recruited axons, and the plateau compound action potential amplitudes indicate full recruitment of available axons. However, as the total number of DRG axons does not increase, it is unlikely that increased compound action potential amplitudes reflect the number of recruited axons (Thakor *et al.*, 2009). Instead, increased compound action potential amplitudes may reflect increased  $\text{Na}^+$  conductance in individual axons due to increased conductance of single channel or an increased number

of  $\text{Na}^+$  channels present in the axonal plasma membrane. In this regard, the  $\beta 2$  subunit increases tetrodotoxin-sensitive  $I_{\text{Na}}$  in small DRG neurons, possibly by promoting cell surface expression of  $\text{Na}_v \alpha$  subunits (Isom *et al.*, 1995; Lopez-Santiago *et al.*, 2006). Similarly, tetrodotoxin-sensitive sodium currents are reportedly increased (Zhang *et al.*, 1997) or unchanged (Berta *et al.*, 2008) in injured small DRG neurons. Taken together, miR-7a-mediated normalization of increased C-fibre compound action potential amplitudes in injured neurons may result in alleviation of neuropathic pain through downregulation of  $\beta 2$  subunit expression.

The mechanisms underlying miR-7a downregulation remain unknown. As miR-7a is encoded in multiple gene loci, it is speculated that multiple signalling pathways intricately regulate miR-7a expression levels. miR-7a expression changes have been reported in diverse cell types and conditions with some conflicting results. In a neuroblastoma cell line, miR-7 expression is downregulated during cell differentiation induced by retinoic acid (Chen *et al.*, 2010), and is also reduced in neurons from Parkinson's disease model mice and glioblastoma (Kefas *et al.*, 2008; Junn *et al.*, 2009; Skalsky and Cullen, 2011). Expression of miR-7 is upregulated by active MAP kinase in a pancreatic cancer cell line (Ikeda *et al.*, 2012), and epidermal growth factor receptor activation stimulates miR-7 expression in an extracellular signal-regulated kinase-dependent manner (Chou *et al.*, 2010). However, in cultured intestinal epithelial cells, miR-7 expression is decreased by interleukin-1 $\beta$ , which potently activates MAP kinases (Nguyen *et al.*, 2010). These lines of evidence offer insight into the complex regulation of miR-7a expression, and clarification of its regulatory mechanisms will lead to further understanding of the pathophysiology of chronic neuropathic pain.

In conclusion, we have shown a pivotal role for miR-7a as a functional RNA in maintenance of neuropathic pain. Notably, miR-7a regulates  $\beta 2$  subunit expression levels, and normalizes neuronal hyperexcitability in neuropathic pain, without affecting physiological and inflammatory pain sensation. Its specific analgesic effects on the late, maintenance phase of neuropathic pain offer a novel therapeutic route, suitable for treatment of neuropathic pain in clinical practice.

## Supplementary material

Supplementary material is available at *Brain* online.

## Acknowledgements

We thank Kumiko Takasu, Kentaro Ohira, Rena Ikeda, Yuka Asaga and Kazusane Takeuchi for their technical assistance, and Takuya Mishima and Toshihiro Takizawa for critical advice on the *in situ* hybridization procedure.

## Funding

This work was supported by a Grant-in-Aid for Encouragement of Young Scientists (B) from the Japan Society for the Promotion of Science (22791457 to A.S.), and a Ministry of Education, Culture,

Sports, Science and Technology-Supported Program for the Strategic Research Foundation at Private Universities, 2008–2012, Japan (S0801035 to H.S.).

## References

- Abdulla FA, Smith PA. Axotomy- and autotomy-induced changes in the excitability of rat dorsal root ganglion neurons. *J Neurophysiol* 2001; 85: 630–43.
- Bai G, Ambalavanar R, Wei D, Dessem D. Downregulation of selective microRNAs in trigeminal ganglion neurons following inflammatory muscle pain. *Mol Pain* 2007; 3: 15.
- Bartel DP. MicroRNAs: target recognition and regulatory functions. *Cell* 2009; 136: 215–33.
- Bennett GJ, Xie YK. A peripheral mononeuropathy in rat that produces disorders of pain sensation like those seen in man. *Pain* 1988; 33: 87–107.
- Berta T, Poirot O, Pertin M, Ji RR, Kellenberger S, Decosterd I. Transcriptional and functional profiles of voltage-gated Na<sup>+</sup> channels in injured and non-injured DRG neurons in the SNI model of neuropathic pain. *Mol Cell Neurosci* 2008; 37: 196–208.
- Chen H, Shalom-Feuerstein R, Riley J, Zhang SD, Tucci P, Agostini M, et al. miR-7 and miR-214 are specifically expressed during neuroblastoma differentiation, cortical development and embryonic stem cells differentiation, and control neurite outgrowth *in vitro*. *Biochem Biophys Res Commun* 2010; 394: 921–7.
- Chou YT, Lin HH, Lien YC, Wang YH, Hong CF, Kao YR, et al. EGFR promotes lung tumorigenesis by activating miR-7 through a Ras/ERK/Myc pathway that targets the Ets2 transcriptional repressor ERF. *Cancer Res* 2010; 70: 8822–31.
- Chung JM, Chung K. Importance of hyperexcitability of DRG neurons in neuropathic pain. *Pain Pract* 2002; 2: 87–97.
- de Chevigny A, Coré N, Follert P, Gaudin M, Barbry P, Béclin C, et al. miR-7a regulation of Pax6 controls spatial origin of forebrain dopaminergic neurons. *Nat Neurosci* 2012; 15: 1120–6.
- Devor M. Sodium channels and mechanisms of neuropathic pain. *J Pain* 2006; 7: S3–S12.
- Fang YX, Xue JL, Shen Q, Chen J, Tian L. MicroRNA-7 inhibits tumor growth and metastasis by targeting the phosphoinositide 3-kinase/Akt pathway in hepatocellular carcinoma. *Hepatology* 2012; 55: 1852–62.
- Friedman RC, Farh KK, Burge CB, Bartel DP. Most mammalian mRNAs are conserved targets of microRNAs. *Genome Res* 2009; 19: 92–105.
- Fukuoka T, Yamanaka H, Kobayashi K, Okubo M, Miyoshi K, Dai Y, et al. Re-evaluation of the phenotypic changes in L4 dorsal root ganglion neurons after L5 spinal nerve ligation. *Pain* 2012; 153: 68–79.
- Gold MS, Gebhart GF. Nociceptor sensitization in pain pathogenesis. *Nat Med* 2010; 16: 1248–57.
- Gonçalves JCR, Oliveira FS, Benedito RB, de Sousa DP, de Almeida RN, de Araújo DAM. Antinociceptive activity of (-)-carvone: evidence of association with decreased peripheral nerve excitability. *Biol Pharm Bull* 2008; 31: 1017–20.
- Güven M, Kahraman I, Koc F, Bozdemir H, Sarica Y, Günay I. The conduction block produced by oxcarbazepine in the isolated rat sciatic nerve: a comparison with lamotrigine. *Neurol Res* 2011; 33: 68–74.
- Hou J, Lam F, Proud C, Want S. Targeting Mnk3 for cancer therapy. *Oncotarget* 2012; 3: 118–31.
- Ikeda Y, Tanji E, Makino N, Kawata S, Furukawa T. MicroRNAs associated with mitogen-activated protein kinase in human pancreatic cancer. *Mol Cancer Res* 2011; 10: 259–69.
- Isom LL, Ragsdale DS, De Jongh KS, Westenbroek RE, Reber BFX, Scheuer T, et al. Structure and function of the  $\beta 2$  subunit of brain sodium channels, a transmembrane glycoprotein with a CAM motif. *Cell* 1995; 83: 433–42.
- Ji RR, Samad TA, Jin SX, Schmolz R, Woolf CJ. p38 MAPK activation by NGF in primary sensory neurons after inflammation increases TRPV1 levels and maintains heat hyperalgesia. *Neuron* 2002; 36: 57–68.
- Ji RR, Strichartz G. Cell signaling and the genesis of neuropathic pain. *Sci STKE* 2004; 2004: re14.
- Junn E, Lee KW, Jeong BS, Chan TW, Im JY, Mouradian MM. Repression of  $\alpha$ -synuclein expression and toxicity by microRNA-7. *Proc Natl Acad Sci USA* 2009; 106: 13052–7.
- Kefas B, Godlewski J, Comeau L, Li Y, Abounader R, Hawkinson M, et al. microRNA-7 inhibits the epidermal growth factor receptor and the Akt pathway and is down-regulated in glioblastoma. *Cancer Res* 2008; 68: 3566–72.
- Kim SH, Chung JM. An experimental model for peripheral neuropathy produced by segmental spinal nerve ligation in the rat. *Pain* 1992; 50: 355–63.
- Kurai T, Hisayasu S, Kitagawa R, Migita M, Suzuki H, Hirai Y, et al. AAV1 mediated co-expression of formylglycine-generating enzyme and aryl-sulfatase A efficiently corrects sulfatide storage in a mouse model of metachromatic leukodystrophy. *Mol Ther* 2007; 15: 38–43.
- Kusuda R, Cadetti F, Ravanelli MI, Sousa TA, Zanon S, De Lucca FL, et al. Differential expression of microRNAs in mouse pain models. *Mol Pain* 2011; 7: 17.
- Lopez-Santiago LF, Pertin M, Morisod X, Chen C, Hong S, Wiley J, et al. Sodium channel  $\beta 2$  subunits regulate tetrodotoxin-sensitive sodium channels in small dorsal root ganglion neurons and modulate the response to pain. *J Neurosci* 2006; 26: 7984–94.
- McNeill E, Van Vactor D. MicroRNAs shape the neuronal landscape. *Neuron* 2012; 75: 363–79.
- Mert T, Gunes Y, Ozcengiz D, Gunay I, Polat S. Comparative effects of lidocaine and tramadol on injured peripheral nerves. *Eur J Pharmacol* 2006; 543: 54–62.
- Nguyen HTT, Dalmaso G, Yan Y, Laroui H, Dahan S, Mayer L, et al. MicroRNA-7 modulates CD98 expression during intestinal epithelial cell differentiation. *J Biol Chem* 2010; 285: 1479–89.
- Niederberger E, Kynast K, Lötsch J, Geisslinger G. MicroRNAs as new players in the pain game. *Pain* 2011; 152: 1455–8.
- Noro T, Miyake K, Suzuki-Miyake N, Igarashi T, Uchida E, Misawa T, et al. Adeno-associated viral vector-mediated expression of endostatin inhibits tumor growth and metastasis in an orthotopic pancreatic cancer model in hamsters. *Cancer Res* 2004; 64: 7486–90.
- O'Connor AB, Dworkin RH. Treatment of neuropathic pain: an overview of recent guidelines. *Am J Med* 2009; 122: S22–32.
- Obata K, Yamanaka H, Fukuoka T, Yi D, Tokunaga A, Hashimoto N, et al. Contribution of injured and uninjured dorsal root ganglion neurons to pain behavior and the changes in gene expression following chronic constriction injury of the sciatic nerve in rats. *Pain* 2003; 101: 65–77.
- Obata K, Yamanaka H, Kobayashi K, Dai Y, Mizushima T, Katsura H, et al. Role of mitogen-activated protein kinase activation in injured and intact primary afferent neurons for mechanical and heat hypersensitivity after spinal nerve ligation. *J Neurosci* 2004; 24: 10211–22.
- Pertin M, Ji RR, Berta T, Powell AJ, Karchewski L, Tate SN, et al. Upregulation of the voltage-gated sodium channel  $\beta 2$  subunit in neuropathic pain models: characterization of expression in injured and non-injured primary sensory neurons. *J Neurosci* 2005; 25: 10970–80.
- Ren K, Dubner R. Interactions between the immune and nervous systems in pain. *Nat Med* 2010; 16: 1267–76.
- Ruggiero V. Involvement of IL-1R/TLR signalling in experimental autoimmune encephalomyelitis and multiple sclerosis. *Curr Mol Med* 2012; 12: 218–36.
- Rutledge EA, Halbert CL, Russell DW. Infectious clones and vectors derived from adeno-associated virus (AAV) serotypes other than AAV type 2. *J Virol* 1998; 72: 309–19.
- Samad OA, Tan AM, Cheng X, Foster E, Dib-Hajj SD, Waxman SG. Virus-mediated shRNA knockdown of Na<sub>v</sub>1.3 in rat dorsal root ganglion attenuates nerve injury-induced neuropathic pain. *Mol Ther* 2013; 21: 49–56.
- Santini E, Huynh TN, MacAskill AF, Carter AG, Pierre P, Ruggiero D, et al. Exaggerated translation causes synaptic and behavioural aberrations associated with autism. *Nature* 2013; 493: 411–15.

- Sayed D, Abdellatif M. MicroRNAs in development and disease. *Physiol Rev* 2011; 91: 827–87.
- Skalsky RL, Cullen BR. Reduced expression of brain-enriched microRNAs in glioblastomas permits targeted regulation of a cell death gene. *PLoS One* 2011; 6: e24248.
- Smith JA, Das A, Ray SK, Banik NL. Role of pro-inflammatory cytokines released from microglia in neurodegenerative diseases. *Brain Res Bull* 2012; 87: 10–20.
- Stys PK, Ransom BR, Waxman SG. Compound action potential of nerve recorded by suction electrode: a theoretical and experimental analysis. *Brain Res* 1991; 546: 18–32.
- Takahashi H, Hirai Y, Migita M, Seino Y, Fukuda Y, Sakuraba H, et al. Long-term systemic therapy of Fabry disease in a knockout mouse by adeno-associated virus-mediated muscle-directed gene transfer. *Proc Natl Acad Sci USA* 2002; 99: 13777–82.
- Takahashi T, Aoki Y, Okubo K, Maeda Y, Sekiguchi F, Mitani K, et al. Upregulation of Ca<sub>v</sub>3.2 T-type calcium channels targeted by endogenous hydrogen sulfide contributes to maintenance of neuropathic pain. *Pain* 2010; 150: 183–91.
- Thakor DK, Lin A, Matsuka Y, Meyer EM, Ruangsri S, Nishimura I, et al. Increased peripheral nerve excitability and local NaV1.8 mRNA up-regulation in painful neuropathy. *Mol Pain* 2009; 5: 14.
- Todd AJ. Neuronal circuitry for pain processing in the dorsal horn. *Nat Rev Neurosci* 2010; 11: 823–36.
- Towne C, Pertin M, Beggah AT, Aebischer P, Decosterd I. Recombinant adeno-associated virus serotype 6 (rAAV2/6)-mediated gene transfer to nociceptive neurons through different routes of delivery. *Mol Pain* 2009; 5: 52.
- von Schack D, Agostino MJ, Murray BS, Li Y, Reddy PS, Chen J, et al. Dynamic changes in the microRNA expression profile reveal multiple regulatory mechanisms in the spinal nerve ligation model of neuropathic pain. *PLoS One* 2011; 6: e17670.
- Woolf CJ, Ma Q. Nociceptors—noxious stimulus detectors. *Neuron* 2007; 55: 353–64.
- Yoon YW, Na HS, Chung JM. Contributions of injured and intact afferents to neuropathic pain in an experimental rat model. *Pain* 1996; 64: 27–36.
- Zhang HY, Zheng SJ, Zhao JH, Zhao W, Zheng LF, Zhao D, et al. MicroRNAs 144, 145, and 214 are down-regulated in primary neurons responding to sciatic nerve transection. *Brain Res* 2011; 1383: 62–70.
- Zhang JM, Donnelly DF, Song XJ, LaMotte RH. Axotomy increases the excitability of dorsal root ganglion cells with unmyelinated axons. *J Neurophysiol* 1997; 78: 2790–4.
- Zhao J, Lee MC, Momin A, Cendan CM, Shepherd ST, Baker MD, et al. Small RNAs control sodium channel expression, nociceptor excitability, and pain thresholds. *J Neurosci* 2010; 30: 10860–71.
- Zhou S, Yu B, Qian T, Yao D, Wang Y, Ding F, et al. Early changes of microRNAs expression in the dorsal root ganglia following rat sciatic nerve transection. *Neurosci Lett* 2011; 494: 89–93.
- Zimmermann M. Ethical guidelines for investigations of experimental pain in conscious animals. *Pain* 1983; 16: 109–10.